ELSEVIER

Catalysis Today 63 (2000) 447–452

CATALYSIS TODAY

www.elsevier.com/locate/cattod

# Active sites in $Cu/ZnO/ZrO_2$ catalysts for methanol synthesis from $CO/H_2$

Young-Woong Suh [a], Seung-Hyun Moon [b], Hyun-Ku Rhee [a,*]

[a] *School of Chemical Engineering and Institute of Chemical Processes, Seoul National University, Kwanak-ku, Seoul 151-742, South Korea*

[b] *District Heating and Cooling Laboratory, Korea Institute of Energy Research, Yousung-ku, Taejon 305-343, South Korea*

**Abstract**

Among various $Cu/ZnO/ZrO_2$ catalysts with the Cu/Zn ratio of 3/7, the one with 15 wt.% of $ZrO_2$ obtains the best activity for methanol synthesis by hydrogenation of CO. The TPR, TPO and XPS analyses reveal that a new copper oxide phase is formed in the calcined $Cu/ZnO/ZrO_2$ catalysts by the dissolution of zirconium ions in copper oxide. In addition, the $Cu/ZnO/ZrO_2$ catalyst with 15 wt.% of $ZrO_2$ turns out to contain the largest amount of the new copper oxide phase. When the $Cu/ZnO/ZrO_2$ catalysts is reduced, the $Cu^{2+}$ species present in the $ZrO_2$ lattice is transformed to $Cu^+$ species. This leads to the speculation that the addition of $ZrO_2$ to Cu/ZnO catalysts gives rise to the formation of $Cu^+$ species, which is related to the methanol synthesis activity of $Cu/ZnO/ZrO_2$ catalyst in addition to Cu metal particles. Consequently, the ratio of $Cu^+/Cu^0$ is an important factor for the specific activity of $Cu/ZnO/ZrO_2$ catalyst for methanol synthesis. © 2000 Elsevier Science B.V. All rights reserved.

*Keywords:* $Cu/ZnO/ZrO_2$ catalyst; Carbon monoxide hydrogenation; Methanol synthesis; $ZrO_2$ effect

## 1. Introduction

Effective synthesis of methanol from $H_2$ and CO has become all the more important in industry, since methanol is considered to be one of the materials that can overcome the forthcoming shortage of petroleum. Industrially, all the methanol is now produced catalytically from synthesis gas containing carbon monoxide, carbon dioxide and hydrogen which is usually produced by steam reforming of natural gas or other hydrocarbons. The copper-containing catalysts such as $Cu/ZnO/Al_2O_3$ and $Cu/ZnO/Cr_2O_3$ have been used at low pressure and temperature.

Also, efforts have been undertaken to enhance the catalytic activity of supported Cu catalysts. In most instances, however, the effect is different depending on the composition of the feed ($CO/H_2$ vs. $CO_2/H_2$). Among various metal oxides, zirconia has attracted much attention because it shows a good activity for both $CO/H_2$ and $CO_2/H_2$ reactions [1–7]. However, attempts to explain how zirconia may influence the methanol synthesis activity of Cu are further clouded by the differences in catalyst preparation and reaction conditions used by different authors. Thus, it remains unclear whether zirconia acts as a textural promoter, a chemical promoter, or a bifunctional catalyst [2].

Despite a number of mechanistic studies, there are still controversies concerning the active species of Cu. On the basis of their opinions on active species of Cu, one may divide the authors into two groups. One group has insisted that the methanol synthesis activity is related linearly to the copper surface area and metallic copper is the active species [8–10]. The other group has claimed that copper metal alone is

---

[*] Corresponding author. Tel.: +82-2-880-7405; fax: +82-2-888-7295.
*E-mail address:* hkrhee@snu.ac.kr (H.-K. Rhee).

PII: S0920-5861(00)00490-9

inactive for carbon monoxide hydrogenation and the amount of $Cu^+$ is related to the methanol synthesis activity over the surface of alkali-doped unsupported Cu catalyst [11–13]. Apart from these two opinions, it is reported that both $Cu^+$ and $Cu^0$ species are essential for methanol formation and the ratio of $Cu^+/Cu^0$ determines the specific activity [14–19]. Okamoto et al. [20] have extensively studied the active species of CuO–ZnO catalysts by means of X-ray photoelectron spectroscopy (XPS) and suggested that the two-dimensional $Cu^0$–$Cu^+$ layer forms active sites for the methanol synthesis at low temperature and pressure.

In the present work, we have prepared a variety of $Cu/ZnO/ZrO_2$ catalysts and examined the catalytic behavior in the hydrogenation of CO to methanol. The XPS characterization was carried out to study the changes of surface copper species induced by the addition of $ZrO_2$. This work was undertaken to provide further insight into the nature of active sites of $Cu/ZnO/ZrO_2$ catalysts.

## 2. Experimental

### 2.1. Sample preparation

Catalyst precursors with various $ZrO_2$ contents were prepared by the coprecipitation method [21]. A volume of 50 ml of 1 M mixed solution containing copper, zinc, and zirconium nitrates (Cu:Zn molar ratio = 3:7) was added dropwise to 100 ml of 1.1 M solution of $NaHCO_3$ at 343 K over a period of 20 min under vigorous stirring, followed by aging for 90 min at the same temperature. The precipitates were filtered and thoroughly washed 10 times with distilled water to remove the residual sodium [22]. The washed precipitates were then dried at 393 K and calcined in air at 623 K for 9 h.

### 2.2. Characterization of catalysts

Powder X-ray diffraction patterns were recorded on a Rigaku D/MAX II-A diffractometer with a Cu target. The reducibility of the metal species is investigated using temperature-programmed reduction (TPR) in a $H_2$ flow. Before TPR experiments, the sample was activated at 673 K in a $N_2$ flow for 1 h. The hydrogen consumption was continuously monitored at a heating rate of 10 K/min in a 15% $H_2/N_2$ stream. The reduced state of bulk catalysts was characterized by temperature-programmed oxidation (TPO). After reducing the catalysts at 573 K for 2 h, thermal gravity (TG) measurements were performed to record TG patterns of the precursor in a flow of 4% $O_2/N_2$ at a heating rate of 10 K/min.

X-ray photoelectron spectra of the catalysts were measured on a Perkin-Elmer PHI 558 using a Mg anode. The catalyst samples were mounted on a double-sided adhesive tape and evacuated to ca. $1\times10^{-5}$ Torr at room temperature in the pretreatment chamber and then transferred to an analyzer chamber maintained at $1 \times 10^{-9}$ Torr. Binding energies were referenced to the $Zn(2p_{3/2})$ level at 1021.7 eV for the catalysts as an internal standard. Since the binding energy (BE) of the $Zn(2p_{3/2})$ level is insensitive to the chemical state, it is known to be suitable for use as an internal standard. The spectra were analyzed in terms of the relative peak area, full width at half maximum (FWHM), chemical shifts in the $Cu(2p_{3/2})$ and $Cu(L_3M_{4,5}M_{4,5})$ Auger levels.

### 2.3. Catalytic activity test

The CO hydrogenation was carried out in a fixed-bed reactor (9.5 mm i.d.) heated by a furnace. The pressure in the reactor was maintained by means of a back pressure regulator and the flow rates of feed gases were controlled by using mass flow controllers. The effluent gas was analyzed by an on-line gas chromatography using Porapak Q column connected to TCD. The product lines were heated electrically to avoid undesired condensation of methanol and water.

Prior to all the experiments, calcined catalysts were reduced in pure $H_2$ flowing at a rate of 50 $cm^3$/min at 523 K for 3 h. The hydrogenation of CO was then carried out at 523 K in a fixed-bed reactor by feeding a gas mixture of $H_2$ and CO with a molar ratio of $H_2/CO = 4$ at a total pressure of 3.45 MPa. Each set of reaction data was obtained averaging several gas chromatographic measurements under steady-state operations. Conversion of CO and methanol selectivity is defined as (number of moles of CO converted to all products)/(number of moles of CO in feedstock) and (number of moles of methanol produced)/(number of moles of CO converted to all products), respectively.

## 3. Results and discussion

Methanol and carbon dioxide were the only carbon-containing products found in this study, except for trace amounts of methane and higher hydrocarbons. The preliminary experiments showed that the Cu/ZnO catalyst with a Cu/Zn ratio of 3/7 has better methanol synthesis activity for CO hydrogenation than the catalyst with any other ratio. This is in accordance with the previous result reported in the literature [21]. Therefore, all the Cu/ZnO/$ZrO_2$ catalysts in this study were prepared with a Cu/Zn ratio of 3/7.

Fig. 1 shows the relationship between the methanol synthesis activity and the content of $ZrO_2$ added to Cu/ZnO catalyst for CO hydrogenation. The maximum yield was obtained when 15 wt.% of $ZrO_2$ was added to Cu/ZnO catalyst. The addition of $ZrO_2$ exhibited a stronger influence on the CO conversion than on the methanol selectivity. For the hydrogenation of $CO_2$, it has been reported that although the specific activity remained unchanged, the addition of $ZrO_2$ increased the dispersion of Cu particle in the catalyst for methanol synthesis [23]. Therefore, it is suggested that the addition of $ZrO_2$ changes the surface area of Cu and adjusts the ratio of $Cu^+/Cu^0$ on the surface of Cu particles to increase the specific activity for CO hydrogenation.

The TPR profiles from Cu/ZnO/$ZrO_2$ catalysts with various $ZrO_2$ contents are presented in Fig. 2. Two peaks are identified, especially for catalysts having $ZrO_2$ contents of 5 and 15 wt.%, respectively. The peak at ca. 473 K represents the reduction of pure or crystalline CuO phase. This is in agreement with the previous report on Cu/ZnO catalyst [24]. The other peak observed at about 423 K indicates that a new CuO phase has been formed. This may have been brought about by the dissolution of zirconium ions in copper oxide phase. The catalyst with 15 wt.% of $ZrO_2$ was found to contain a large amount of the new CuO phase and give the maximum yield of methanol. Therefore, it is evident that the new CuO phase is closely related to the methanol synthesis activity.

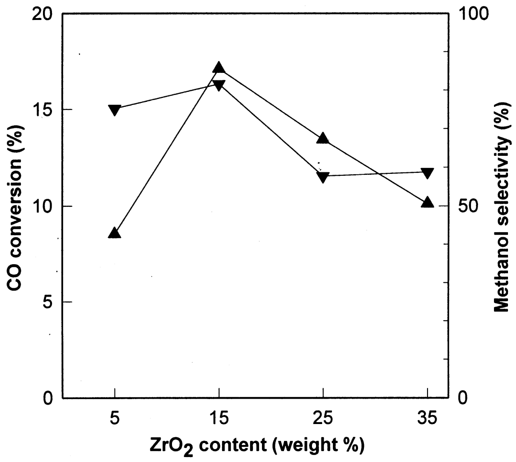

Fig. 1. Effect of $ZrO_2$ content in Cu/ZnO/$ZrO_2$ catalysts on CO conversion (▲) and methanol selectivity (▼), respectively.

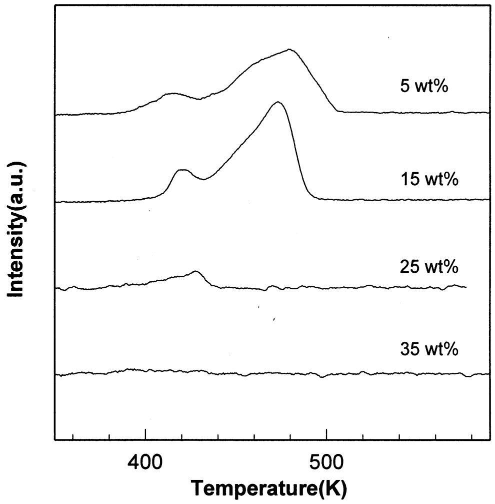

Fig. 2. TPR profiles of Cu/ZnO/$ZrO_2$ catalysts with various $ZrO_2$ contents.

Fig. 3 presents the TPO patterns of Cu/ZnO catalyst and Cu/ZnO/$ZrO_2$ catalysts with various $ZrO_2$ contents. Here, the weight increment determined by TG indicates that the transformation of $Cu^0$ to $Cu^{2+}$ occurs during the entire period of heating. According to Li and Inui [25], TPO profiles are mainly composed of three peaks. The low-temperature peak in the range 373–433 K and the high-temperature peak above 473 K correspond to the conversion of $Cu^0$ to $Cu^+$ and $Cu^+$ to $Cu^{2+}$, respectively, whereas the intermediate-temperature peak in the range 433–473 K represents the transformations of $Cu^0$ in a hard-oxidized state to $Cu^+$ and $Cu^+$ in an easily oxidized state to $Cu^{2+}$. This indicates that the intermediate-temperature peak is related to

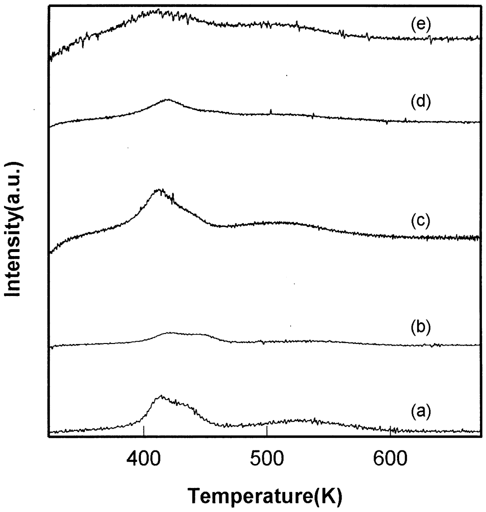

Fig. 3. TPO patterns of (a) Cu/ZnO catalyst and Cu/ZnO/$ZrO_2$ catalysts with $ZrO_2$ contents of (b) 5 wt.%, (c) 15 wt.%, (d) 25 wt.%, (e) 35 wt.%, respectively.

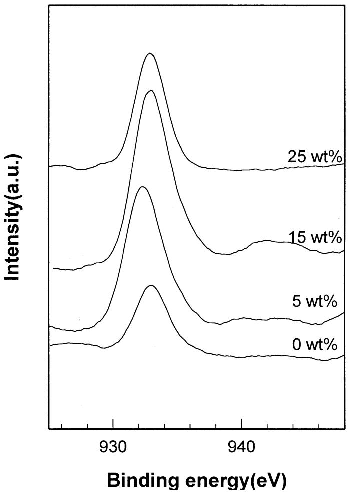

Fig. 4. Cu($2p_{3/2}$) X-ray photoelectron spectra of calcined CuO/ZnO/$ZrO_2$ catalysts with various contents of $ZrO_2$.

$Cu^+$, which is an important factor for the activity of methanol synthesis.

The result of quantitative analysis of all TPO patterns is presented in Table 1. The area of each peak is calculated by Gaussian curve fitting and the area ratio between each of the Cu/ZnO/$ZrO_2$ catalysts and the Cu/ZnO catalyst is obtained. Clearly, the Cu/ZnO/$ZrO_2$ catalyst with 15 wt.% of $ZrO_2$ has the largest area ratio in the intermediate-temperature peak. In other words, $Cu^+$ is present most abundantly in this catalyst. This suggests that $Cu^+$ is closely related to the methanol synthesis activity and further that there may exist an optimum ratio of $Cu^+$ to $Cu^0$.

Table 1
Results of TPO data analysis of Cu/ZnO catalyst and Cu/ZnO/$ZrO_2$ catalysts with various contents of $ZrO_2$[a]

| | CZ37[b] | CZZ3705[b] | CZZ3715[b] | CZZ3725[b] |
|---|---|---|---|---|
| Weight, *W* (mg) | 7.987 | 4.182 | 17.452 | 10.875 |
| Area of LTP[c]/*W* | 0.0255 | 0.024 | 0.027 | 0.023 |
| Area of ITP[c]/*W* | 0.007 | 0.006 | 0.012 | 0.005 |
| Area of HTP[c]/*W* | 0.025 | 0.035 | 0.036 | 0.029 |
| CZZ37x/CZ37 of LTP (a) | 1 | 0.941 | 1.059 | 0.902 |
| CZZ37x/CZ37 of ITP (b) | 1 | 0.857 | 1.714 | 0.714 |
| (b)/(a) | 1 | 0.911 | 1.619 | 0.792 |

[a] Area calculation: Gaussian curve fitting by graphic software.

[b] 37: mole ratio of Cu and ZnO = 3/7; 05, 15, 25: $ZrO_2$ contents of Cu/ZnO/$ZrO_2$ catalysts.

[c] LTP/ITP/HTP: low/intermediate/high temperature peak.

The XPS spectra of the Cu($2p_{3/2}$) levels for the calcined Cu/ZnO and Cu/ZnO/$ZrO_2$ catalysts are shown in Fig. 4. The XPS parameters for the catalysts are summarized in Table 2. As a result of measuring Zr($3d_{3/2}$ and $3d_{5/2}$) spectra for calcined Cu/ZnO/$ZrO_2$ catalysts, Zr($3d_{3/2}$) peak and Zr($3d_{5/2}$) peak were found invariant under the addition of $ZrO_2$. Therefore, no particular information about the bonding nature of $Zr^{4+}$ ions is obtained solely from the core BE. On the other hand, the change of $Cu^{2+}$ ions was observed with the addition of $ZrO_2$. In particular, the FWHM value of Cu($2p_{3/2}$) satellite peak increases with the amount of $ZrO_2$ in the Cu/ZnO/$ZrO_2$ catalyst and this provides information about the bonding nature of $Cu^{2+}$ ion in the catalyst.

For the calcined catalysts, the BE of the Cu($2p_{3/2}$) level was practically invariant with the catalyst composition. It is well known that the first transition metal ions which have unfilled 3d orbitals show well-separated satellite peaks in the core level XPS spectra due to the electron shake-up and the satellite structure reflects the nature of chemical bonding of the transition metal ions [26]. Accordingly, a closer examination of shake-up satellites or FWHM of the Cu($2p_{3/2}$) parent peak was performed.

Table 2
XPS BE and kinetic energy (KE) and XPS satellite structure of the Cu($2p_{3/2}$) level for the reduced Cu/ZnO/$ZrO_2$ catalysts[a]

| $ZrO_2$ content (wt.%) | BE of Cu($2p_{3/2}$) level (eV) | KE (eV) | | BE of O(1s) level (eV) | FWHM[c] (eV) | | $I_s/I_p$[d] |
|---|---|---|---|---|---|---|---|
| | | Cu(LMM)[b] level | Zn(LMM)[b] level | | Parent | Satellite | |
| 0 | 932.7 | 918.2 | 988.2 | 530.5 | 2.9 | 4.4 | nd[e] |
| 5 | 932.6 | 917.5 | 988.8 | 530.7 | 3.3 | 4.6 | 0.24 |
| 15 | 932.0 | 916.5 | 989.0 | 531.4 | 3.7 | 5.7 | 0.20 |
| 25 | 932.5 | 917.3 | 988.1 | 531.1 | 2.8 | nd[e] | nd[e] |

[a] Referenced to the Zn($2p_{3/2}$) level (1021.7 eV).
[b] LMM represents $L_3M_{4,5}M_{4,5}$.
[c] Full width at half maximum.
[d] $I_s$ and $I_p$ show the area intensities of satellite and parent peaks, respectively.
[e] Not determined.

In the case of CuO, the $Cu^{2+}$ ion is surrounded by four oxygen anions in a nearly square-planar symmetry. When the symmetry of $Cu^{2+}$ ion in a square-planar arrangement is slightly distorted in CuO, other charge-transfer excitations may become allowed due to electron correlation effects [20]. The broad shake-up satellite structure for pure CuO is considered to be a consequence of a slight distortion of the $D_{4h}$ symmetry. As presented in Table 2, the FWHM value of parent peaks is changed with the addition of $ZrO_2$ and the catalyst with 15 wt.% of $ZrO_2$ has the largest FWHM value in parent structure. Therefore, it is speculated that the presence of $ZrO_2$ causes the coordination symmetry of $Cu^{2+}$ ions in CuO to be distorted presumably toward a highly distorted octahedral symmetry by forming weak additional $Cu^{2+}$–$Cu^{2-}$ bondings with neighboring or extra $O^{2-}$ ions. Also, the catalyst with 15 wt.% of $ZrO_2$ has the largest amount of distorted $Cu^{2+}$ ions.

The X-ray photoelectron spectra of the Cu($L_3M_{4,5}$ $M_{4,5}$) Auger line for the reduced catalysts are shown in Fig. 5. The distinction between $Cu^+$ and $Cu^0$ cannot be made solely on the basis of the BE of the Cu($2p_{3/2}$) level, but it is evident that there is a shoulder peak at a lower energy side (916.7 eV) of the principal Auger line ascribed to the metallic copper as shown in Fig. 5. According to the previous report [20], the shoulder peak observed at 916.7 eV is attributed to $Cu^+$ species. This $Cu^+$ species seems to be produced by the reduction of $Cu^{2+}$ ions in a distorted octahedral symmetry. From the X-ray photoelectron spectra of the calcined Cu/ZnO/$ZrO_2$ catalysts, the largest shoulder peak is observed in the case of the catalyst having 15 wt.% of $ZrO_2$.

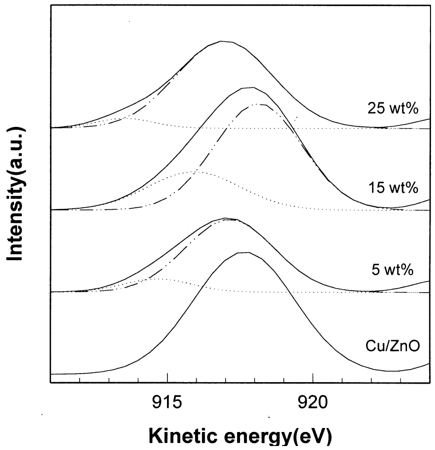

Fig. 5. Cu($L_3M_{4,5}M_{4,5}$) Auger spectra for reduced Cu/ZnO/$ZrO_2$ catalysts with various contents of $ZrO_2$: (—) original spectra, (—··—) principal peak, (···) shoulder peak.

## 4. Conclusions

Cu/ZnO/$ZrO_2$ catalysts are found to show a good activity for the methanol synthesis at low temperature and pressure. Among Cu/ZnO/$ZrO_2$ catalysts with a Cu/Zn molar ratio of 3/7, the highest activity was obtained with the one containing 15 wt.% of $ZrO_2$. Bulk characterization of catalysts revealed the presence of a new copper oxide phase that was formed by the dissolution of zirconium ions in the copper oxide phase.

The result of XPS analysis of the calcined catalysts confirms that the copper oxide species is formed by a distortion of the square-planar symmetry of pure CuO toward an octahedral symmetry. When the catalyst is reduced, the distorted $Cu^{2+}$ ions are converted to $Cu^{+}$ ions. The $Cu/ZnO/ZrO_2$ catalyst with 15 wt.% of $ZrO_2$ turns out to contain the largest amount of the new copper oxide phase. Consequently, $Cu^{+}$ ions may be considered as the active sites for the methanol synthesis reaction. It is evident that the addition of $ZrO_2$ promotes the formation of $Cu^{+}$ ions and the ratio of $Cu^{+}/Cu^{0}$ plays a central role in the $Cu/ZnO/ZrO_2$ catalyst with 15 wt.% of $ZrO_2$.

## References

[1] Y. Nitta, O. Suwata, Y. Ikeda, Y. Okamoto, T. Imanaka, Catal. Lett. 26 (1994) 345.
[2] I.A. Fischer, H.C. Woo, A.T. Bell, Catal. Lett. 44 (1997) 11.
[3] I.A. Fischer, A.T. Bell, J. Catal. 178 (1998) 153.
[4] Y. Liu, B. Zhong, S. Peng, Q. Wang, T. Hu, Y.N. Xie, X. Ju, Catal. Today 30 (1996) 177.
[5] J. Weigel, C. Frohlich, A. Baiker, A. Wokaun, Appl. Catal. A 140 (1996) 29.
[6] J. Wu, S. Luo, J. Toyir, M. Saito, M. Takeuchi, T. Watanabe, Catal. Today 45 (1998) 215.
[7] Z. Liu, W. Ji, L. Dong, Y. Chen, J. Catal. 172 (1997) 243.
[8] G.C. Chinchen, K.C. Waugh, D.A. Whan, Appl. Catal. 25 (1986) 101.
[9] G.C. Chinchen, K.C. Waugh, J. Catal. 97 (1986) 280.
[10] P.B. Rasmussen, M. Kazuta, I. Chorkendorff, Surf. Sci. 318 (1994) 267.
[11] G.R. Sheffer, T.S. King, J. Catal. 115 (1989) 376.
[12] G.R. Sheffer, T.S. King, J. Catal. 116 (1989) 488.
[13] V. Ponec, Surf. Sci. 272 (1992) 111.
[14] R.G. Herman, K. Klier, G.W. Simmons, B.P. Finn, J.B. Bulko, T.P. Kobylinski, J. Catal. 56 (1979) 407.
[15] T. Fujitani, M. Saito, Y. Kanai, T. Kakumoto, T. Watanabe, J. Nakamura, T. Uchijima, Catal. Lett. 25 (1994) 271.
[16] T. Fujitani, I. Nakamura, T. Watanabe, T. Uchijima, J. Nakamura, Catal. Lett. 35 (1995) 297.
[17] J. Nakamura, I. Nakamura, T. Uchijima, Y. Kanai, T. Watanabe, M. Saito, T. Fujitani, Catal. Lett. 31 (1995) 325.
[18] J. Nakamura, T. Uchijima, Y. Kanai, T. Fujitani, Catal. Today 28 (1996) 223.
[19] Y. Kanai, T. Watanabe, T. Fujitani, T. Uchijima, J. Nakamura, Catal. Lett. 38 (1996) 157.
[20] Y. Okamoto, K. Fukino, T. Imanaka, S. Teranishi, J. Phys. Chem. 87 (1983) 3740.
[21] S. Fujita, A.M. Satriyo, G.C. Shen, N. Takezawa, Catal. Lett. 34 (1995) 85.
[22] K.-W. Jun, W.-J. Shen, K.S.R. Rao, K.-W. Lee, Appl. Catal. A 174 (1998) 231.
[23] M. Saito, T. Fujitani, M. Takeuchi, T. Watanabe, Appl. Catal. A 138 (1996) 311.
[24] G. Fierro, M.L. Jacono, M. Inversi, P. Porta, R. Lavecchia, F. Cioci, J. Catal. 148 (1994) 709.
[25] J.-L. Li, T. Inui, Appl. Catal. A 137 (1996) 105.
[26] T.A. Carlson, Photoelectron and Auger Spectroscopy, Plenum Press, New York, 1975.